

Anisotropic tensor power spectrum at interferometer scales induced by tensor squeezed non-Gaussianity

Angelo Ricciardone¹, Gianmassimo Tasinato²

¹ *Faculty of Science and Technology, University of Stavanger, 4036, Stavanger, Norway*

² *Department of Physics, Swansea University, Swansea, SA2 8PP, U.K.*

Abstract

We develop a scenario of inflation with spontaneously broken time and space diffeomorphisms, with distinctive features for the primordial tensor modes. Inflationary tensor fluctuations are non adiabatic, and can acquire a mass during the inflationary epoch. They can evade the Higuchi bound around de Sitter space, thanks to interactions with the fields driving expansion. Correspondingly, the primordial stochastic gravitational wave background (SGWB) is characterised by a tuneable scale dependence, and can be detectable at interferometer scales. In this set-up, tensor non-Gaussianity can be parametrically enhanced in the squeezed limit. This induces a coupling between long and short tensor modes, leading to a specific quadrupolar anisotropy in the primordial SGWB spectrum, which can be used to build estimators for tensor non-Gaussianity. We analyse how our inflationary system can be tested with interferometers, also discussing how an interferometer can be sensitive to a primordial anisotropic SGWB.

Contents

1	Introduction	1
2	Set-up and symmetries	2
3	Background solutions and cosmological fluctuations	4
3.1	First step: spontaneous breaking of time reparameterization	4
3.2	Second step: spontaneous breaking of time and space reparameterizations	6
4	Phenomenological consequences	9
4.1	Tensor blue spectrum: inflationary tensor modes at interferometers	9
4.2	Tensor squeezed non-Gaussianity and anisotropic tensor power spectrum	11
4.3	Interferometer response to an anisotropic tensor power spectrum	13
5	Discussion	16
A	ADM constraints for scalar perturbations	17

1 Introduction

Cosmological inflation predicts the existence of a stochastic background of gravitational waves (SGWB), whose power spectrum amplitude depends on the value of the Hubble parameter during inflation, as well as on the details of the inflationary process: see [1, 2] for reviews. In most inflationary models, the tensor power spectrum is almost scale invariant, with a slightly red tensor tilt. In this case, the most promising way to detect the primordial SGWB is through Cosmic Microwave Background (CMB) B-mode polarisation (see e.g. [3]). There are however examples of inflationary scenarios where the amplitude of tensor modes can be amplified at scales much smaller than CMB's (see e.g. [4–8]). These frameworks are observationally interesting, since they open the possibility for gravitational wave interferometers to probe the primordial SGWB, and to constrain inflationary models; see e.g. [9] for a study on the capabilities of the future Laser Interferometer Space Antenna (LISA) in this respect, containing the relevant references to the original literature.

Among the different scenarios which show interesting features for gravitational waves (GW) at small scales, here we focus on a generalisation of solid inflation [10, 11] dubbed supersolid inflation [12, 13]. This scenario explores the possibility of breaking both time and space diffeomorphisms during the inflationary epoch, by means of space-dependent *vacuum expectation values* (*vevs*) of the set of scalar fields that drive inflation. Such a symmetry breaking pattern makes the primordial tensor modes non adiabatic: this implies that tensor fluctuations acquire a mass during inflation, and this affects the tensor power spectrum [14]. In the original set-up [10], a blue tensor spectrum was also found, with positive tensor spectral tilt proportional to the inflationary slow-roll parameter.

In this work we show that, within the context of supersolid inflation, it is possible to build concrete models with parametrically larger positive values for the tensor spectral tilt. We can obtain this feature by including appropriate non-minimal couplings between gravity and the scalar fields driving inflation.

One of the first results is that we evade the Higuchi bound [15, 16] in a de Sitter space, since the time and space-dependent *vevs* of the scalar fields break the de Sitter isometries that are needed for the applicability of Higuchi theorem. A blue spectrum for tensor modes leads to a tensor power spectrum which increases at small scales, and the amplitude of SGWB can be sufficiently large to be detectable at scales probed by interferometer. We discuss how LISA can probe a region of parameter space of supersolid inflation models, and test their predictions for the amplitude of the inflationary tensor spectrum.

In [17] we shown that supersolid inflation can lead to parametrically large tensor non-Gaussianity (nG) enhanced in the squeezed limit. The symmetry breaking pattern we analyse make the tensors non-adiabatic, and Maldacena’s consistency relation on the squeezed limit of the tensor three-point (3-pt) function [18] can be violated. In this work, we study how a large squeezed tensor nG leads to a quadrupolar anisotropy in the tensor power spectrum, induced by the coupling between long and short (wavelength) tensor modes. We discuss how the amplitude of the anisotropic contribution to the tensor power spectrum can be used to build estimators for tensor non-Gaussianity. We also start to analyse the consequences of an anisotropic primordial SGWB for interferometers, and in particular we analyse how the response function of the instrument behaves in presence of such an anisotropic signal.

The structure of the paper is the following: Section 2 discusses the supersolid set-up under consideration and the symmetries that dictate such a system. In Section 3 we study the background evolution in two steps. We first analyze the dynamics of gravity non-minimally coupled to a single time-dependent scalar field; then we consider both time and space-dependent background fields and we study the features of corresponding primordial cosmological fluctuations. In Section 4 we analyse phenomenological implications of our findings and we compute the response of an interferometer to a primordial anisotropic SGWB. We conclude in Section 5 where we summarize our results and discuss possible future developments. In Appendix A we present the equations for the Arnowitt-Deser-Misner (ADM) constraints [19].

2 Set-up and symmetries

The action

We analyse a system whose field content and interactions lead to a space-time symmetry breaking pattern with novel features for the inflationary tensor spectrum.

We are interested in a cosmological framework where both time and space reparameterization symmetries are spontaneously broken by vacuum expectation values of scalar fields [12, 13]. Such system is a generalization of solid inflation [10], where three derivatively coupled scalar fields have space-dependent background values. For definiteness, we take as cosmological background de Sitter space-time; although it does not represent a realistic inflationary set-up (inflation should end at some time, while de Sitter inflationary expansion does not stop), nevertheless it is convenient for our discussion, which focuses specifically on the dynamics of primordial tensor modes.

Our field content includes gravity and a quartet of scalar fields, ϕ and σ^I ($I = 1, 2, 3$), responsible for breaking space-time diffeomorphisms. As we shall discuss, our action is motivated by symmetry considerations, and it reads as

$$S = \int d^4x \sqrt{-g} [\mathcal{L}_R - \mathcal{L}_\phi - M_{Pl}^4 \mathcal{L}_\sigma] , \quad (2.1)$$

with

$$\mathcal{L}_R = \frac{M_{Pl}^2}{2} R, \quad (2.2)$$

$$\mathcal{L}_\phi = \frac{1}{2} \partial_\mu \phi \partial^\mu \phi + V_0 + \frac{q_\phi}{M_{Pl}^2} G^{\mu\nu} \partial_\mu \phi \partial_\nu \phi, \quad (2.3)$$

$$\mathcal{L}_\sigma = q_A F(\phi) \text{Tr}(B) + q_B F^2(\phi) \text{Tr}(B^2) + \lambda_0^2 q_C \frac{\text{tr}(B^2)}{(\text{Tr}B)^2} + \frac{q_\sigma}{M_{Pl}^2} F(\phi) \delta_{IJ} \partial_\mu \sigma^I \partial_\nu \sigma^J G^{\mu\nu}, \quad (2.4)$$

where $G^{\mu\nu}$ is the Einstein tensor, the Greek indices $\mu, \nu = 0, 1, 2, 3$ denote spacetime coordinates, V_0 is a constant potential, q_i and λ_0 are dimensionless parameters and M_{Pl} is the Planck mass. The scalar field ϕ has dimension of a mass, while the fields σ^I have dimension of inverse of a mass. With ‘‘Tr’’ we indicate the trace of the field matrix B_{IJ} which is defined as

$$B_{IJ} \equiv \partial_\mu \sigma_I \partial^\mu \sigma_J, \quad I, J = 1, 2, 3. \quad (2.5)$$

We choose the function $F(\phi)$ as

$$F(\phi) = \exp[2H_0 \phi / \kappa_0^2], \quad (2.6)$$

where the two positive parameters H_0 and κ_0 have dimension of a mass. These two parameters play a special role in characterising the background configurations. The scalar field ϕ acquires a time-dependent background profile $\phi(t)$ which spontaneously break time reparameterization [20]; the triplet of scalars σ^I have space dependent *vevs* breaking space reparameterization. Interactions of ϕ and σ^I are described by the Lagrangians \mathcal{L}_ϕ and \mathcal{L}_σ which include non-minimal couplings with gravity, described by operators proportional to $G_{\mu\nu} \partial^\mu \phi \partial^\nu \phi$ and $G_{\mu\nu} \partial^\mu \sigma^I \partial^\nu \sigma^J \delta_{IJ}$. Such non-linear derivative interactions belong to the family of Horndeski scalar-tensor theories [21], and have been first applied to inflation in [22, 23]. They are ghost free and do not lead to Ostrogradsky instabilities. We should *not* think to them as small corrections to the leading two derivative operators controlled by the kinetic terms. Instead we exploit their structure and focus on branches of cosmological background configurations where their effects are particularly relevant.

Action (2.1) enriches the system examined in [17] by including the operators $G^{\mu\nu} \partial_\mu \phi \partial_\nu \phi$, as well as operators quadratic in B_{IJ} . As we shall see, these contributions are important for characterizing the evolution of tensor modes during inflation, in particular to avoid the Higuchi bound, to get a parametrically large positive tensor tilt, and enhanced tensor non-Gaussianity in the squeezed limit, which induces a quadrupolar anisotropy in the power spectrum.

Symmetries

The structure of action (2.1) is dictated by symmetry considerations, which we discuss here. We only consider covariant operators with up to four derivatives. In section 3, we analyse background solutions of field equations which spontaneously break space-time isometries through *vevs* for scalar fields. On the other hand, we recover these space-time symmetries at the background level by imposing internal shift and rotational symmetries for the fields. We impose a shift internal symmetry for each of the four scalars involved:

$$\phi \rightarrow \phi + c^0, \quad (2.7)$$

$$\sigma^I \rightarrow \sigma^I + c^I, \quad (2.8)$$

where c^0, c^I are constants. Moreover, the three scalars σ^I satisfy an internal rotational symmetry

$$\sigma^I \rightarrow \Lambda^I{}_J \sigma^J, \quad (2.9)$$

where the constant matrix $\Lambda^I{}_J \in SO(3)$, similar to the case of solid inflation [10]. Such internal symmetries allow one to recover the space-time symmetries spontaneously broken by scalar *vevs*, and ensure isotropy and homogeneity for the geometrical background in accordance with observational CMB evidences [24].

Additionally, we also impose an internal scaling symmetry, distinctive of a scenario of supersolid inflation [17, 25]

$$\sigma^I \rightarrow \ell \sigma^I, \quad (2.10)$$

$$\phi \rightarrow \phi - \frac{\kappa_0^2}{H_0} \ln(\ell), \quad (2.11)$$

for some constant scaling parameter ℓ . This scaling symmetry constrains the possible four-derivative operators involving the scalars σ^I to the ones appearing in action (2.1), and motivates the structure of the exponential coupling functions between ϕ and the scalar triplet σ^I . The scaling symmetry (2.10), together with rotational symmetry (2.9), are relevant for characterizing properties of the fluctuations [25], as we will discuss in the next Section.

3 Background solutions and cosmological fluctuations

We consider background configurations where the scalar fields spontaneously break time and space reparameterizations due to non-vanishing *vevs*. We focus on a de Sitter geometry for the background, a space-time of sufficient generality to analyse features of primordial tensor modes:

$$ds^2 = -dt^2 + e^{2H_0 t} d\vec{x}^2, \quad (3.1)$$

where H_0 is the Hubble parameter during the de Sitter phase. It is instructive to break space-time isometries in steps, so to appreciate the consequences of each class of operators contained in \mathcal{L}_ϕ and \mathcal{L}_σ .

3.1 First step: spontaneous breaking of time reparameterization

We start considering a “reduced” action with respect to (2.1), only describing the dynamics of gravity non-minimally coupled with a single scalar field ϕ

$$S = \int d^4x \sqrt{-g} [\mathcal{L}_R - \mathcal{L}_\phi], \quad (3.2)$$

with $\mathcal{L}_R, \mathcal{L}_\phi$ given in (2.2) and (2.3) respectively. Such action is an example of quartic Horndenski Lagrangian. Applications to cosmological inflation of Horndenski-type couplings, as the ones above, have been much studied in the literature, starting with [22, 23, 26, 27].

The background geometry is de Sitter space, (3.1), while we take the following homogeneous time-dependent ansatz for the scalar ϕ

$$\phi = \kappa_0^2 t, \quad (3.3)$$

with κ_0 the same parameter appearing in the the function $F(\phi)$ in eq (2.6). Notice that if κ_0 is non-vanishing, then the scalar *vev* spontaneously breaks time reparameterization: $\phi(t + \Delta t) \neq \phi(t)$.

Due to non-minimal coupling with gravity and the non-linearity of the equations, the system admits two distinct branches of de Sitter solutions, given by

- **Branch 1**

$$H_0^2 = \frac{V_0}{3M_{Pl}^2}, \quad (3.4)$$

$$\kappa_0 = 0. \quad (3.5)$$

- **Branch 2**

$$H_0^2 = \frac{M_{Pl}^2}{6q_\phi}, \quad (3.6)$$

$$\kappa_0^4 = \frac{2q_\phi V_0 - M_{Pl}^4}{2q_\phi}. \quad (3.7)$$

We are interested on the second branch, where the rate of expansion is inversely proportional to the parameter q_ϕ controlling the non-minimal coupling between the scalar field and gravity. Parameterising the constant potential V_0 in terms of a quantity v_1 as

$$V_0 = 3H_0^2 M_{Pl}^2 + 2 M_{Pl}^2 v_1^2, \quad (3.8)$$

and using (3.6), then eq (3.7) becomes simpler

$$\kappa_0^4 = 2M_{Pl}^2 v_1^2. \quad (3.9)$$

Hence the parameter v_1 controls the breaking of time-reparameterisation in this system. If $v_1 = 0$, then $\kappa_0 = 0$, and the two branches of solutions coincide.

The dynamics of cosmological fluctuations around the background solution depends on the symmetry breaking parameter v_1 . We analyse the quadratic actions for scalar and tensor fluctuations following closely the methods we implemented in [17], to which we refer the reader for more details. We choose an unitary gauge for scalar fluctuations, where the scalar ϕ is unperturbed, while the metric fluctuations read (see also [28])

$$ds^2 = -(1 + 2N) dt^2 + 2 e^{2H_0 t} \partial_i B dx^i dt + e^{2H_0 t} (1 + 2A) \delta_{ij} dx^i dx^j. \quad (3.10)$$

The equations of motion for the scalar quantities N and B , which are not dynamical, lead to the lapse and shift constraints [29]. After imposing these constraint conditions, we find the following quadratic action for the scalar fluctuation A , the only scalar mode that propagates:

$$S_A^{(2)} = \left[\frac{4 v_1^4 (v_1^2 + 3H_0^2)}{9H_0^2 (v_1^2 + H_0^2)^2} \right] \times \int dt d^3x a^3 \left(\dot{A}^2 - \frac{c_A^2}{a^2} (\nabla A)^2 \right), \quad (3.11)$$

where c_A is the sound speed of the scalar fluctuation A

$$c_A^2 = \frac{v_1^2 + H_0^2}{v_1^2 + 3H_0^2}. \quad (3.12)$$

The overall coefficient in S_A is proportional to a power of v_1 , controlling the time dependent vev of the scalar field profile. The scalar fluctuation A can be thought as the Goldstone boson associated with the

spontaneous breaking of time reparameterization, and acquires non-trivial dynamics when $v_1 \neq 0$, and hence the scalar profile $\phi(t)$ is turned on.

When we pass to consider the tensor sector it is convenient to parameterize it as [29]

$$ds^2 = -dt^2 + a^2(t) (\delta_{ij} + \hat{\gamma}_{ij}) dx^i dx^j, \quad (3.13)$$

where $a(t)$ is the scale factor during the de Sitter phase, and $\hat{\gamma}$ can be expanded as

$$\hat{\gamma}_{ij} = \gamma_{ij} + \frac{1}{2}\gamma_{ik}\gamma_{kj} + \frac{1}{6}\gamma_{ik}\gamma_{kl}\gamma_{lj}, \quad (3.14)$$

where γ_{ij} represents a first order, transverse ($\partial_i\gamma_j^i = 0$) and traceless ($\gamma_i^i = 0$) tensor fluctuation. The quadratic action for tensor modes around the de Sitter background configuration results

$$S_\gamma^{(2)} = \frac{M_{Pl}^2 (v_1^2 + 3H_0^2)}{12H_0^2} \int dt d^3x a^3 \left(\dot{\gamma}_{ij} - \frac{c_T^2}{a^2} (\nabla\gamma_{ij})^2 \right), \quad (3.15)$$

where c_T represents the tensor sound speed

$$c_T^2 = \frac{3H_0^2 - v_1^2}{3H_0^2 + v_1^2}. \quad (3.16)$$

Action (3.15) depends on the symmetry breaking parameter v_1 , both for what respect the effective Planck mass, which gets “renormalised” (see the coefficient in front of eq (3.15)), and the tensor sound speed, see eq (3.16). When $v_1 = 0$, one recovers the standard General Relativity (GR) result for tensor fluctuations around de Sitter space [30].

The breaking of time reparameterization – and the direct coupling between tensor fluctuations and the fields driving inflation – lead to a distinct behaviour for tensor fluctuations in this set-up, even around a pure de Sitter geometry ¹. More drastic consequences occur to tensor perturbations when breaking also space isometries, as we are going to discuss in the next subsection.

3.2 Second step: spontaneous breaking of time and space reparameterizations

We proceed by considering a more general set-up, spontaneously breaking all space-time isometries by the *vevs* of scalar fields, including also space reparameterizations. The total action that we now analyse includes the fields σ^I , and reads as in eq (2.1). The background profiles for ϕ and σ^I which solve the background equations of motion are

$$\phi = \kappa_0^2 t, \quad (3.17)$$

$$\sigma^I = \lambda_0 x^I, \quad I = 1, 2, 3, \quad (3.18)$$

with the parameters κ_0 breaking time reparameterizations, while λ_0 breaking space reparameterizations (as in [17]). The geometry is de Sitter space, with metric ansatz given by (3.1). This system is a generalization of solid inflation [10] to a supersolid set-up [13, 17], where we break both time and space reparameterization invariance during inflation. The number of degrees of freedom generically changes:

¹ Notice that the tensor sound speed might be set to one through a disformal transformation [31–33], but this does not modify any physical consequences of the system since physical quantities do not depend on the frame [32]. We will not need to consider such disformal transformation in the present context.

since we break further symmetries, a new scalar excitation is expected to propagate, which we call ω , corresponding to the Goldstone boson for broken space reparameterization. Such a quantity is associated with a perturbation of the field σ^I :

$$\sigma^I = \lambda_0 x^I + \frac{\lambda_0}{\sqrt{-\nabla^2}} \omega^I, \quad (3.19)$$

with $\omega^I = \hat{\omega}^I + \partial^I \omega$ (the former a vector, the latter the scalar fluctuation we are discussing). On the other hand, our system is equipped with the scaling symmetry (2.10), that was shown in [25] to forbid the propagation of ω at large scales. The argument, which we borrow from [25], can be summarized as follows: at large scales, we can parameterize the configuration for ω^I as

$$\omega^I = a \delta^I_J x^J + b^{IJ} \delta_{JM} x^M, \quad (3.20)$$

where a, b^{IJ} are slowly varying in space, and b is antisymmetric in its indexes. The first term proportional to a in eq (3.20) is associated with a scalar mode, while the term proportional to b^{IJ} corresponds to a vector mode. However these fluctuations can be reabsorbed by an infinitesimal symmetry transformation that combines rotational (2.9) with scale (2.10) invariance. Hence, the mode ω^I does not acquire dynamics, at least at large scales, being a pure gauge for the system under consideration.

The dynamics of ω at smaller scales can be in principle taken into full account, as done in [13, 17], but gives only subleading contributions to the physics of the scalar sector at large scales. Since our work mostly focuses on the dynamics of tensor modes, for simplicity we choose the available parameters such that ω does not propagate at all at quadratic level (i.e. its quadratic action has vanishing overall coefficient). This amounts to select parameters such that the following relation is satisfied

$$q_\phi q_\sigma = (q_A + 2q_B \lambda_0^2), \quad (3.21)$$

and we assume in what follows that both q_ϕ and q_σ are non-vanishing².

We choose a branch among the possible background solutions, where the value of the Hubble parameter is controlled by the parameters q_i , ($i = \phi, \sigma$), generalizing the results of Section 3.1. The background equations are solved by the following values of H_0, κ_0 (together with condition (3.21)):

$$H_0^2 = \frac{M_{Pl}^2}{6 q_\sigma} (q_A + 2q_B \lambda_0^2), \quad (3.22)$$

$$\kappa_0^4 = \frac{M_{Pl}^4}{6} \lambda_0^2 (q_C - 9q_B \lambda_0^2) + 2M_{Pl}^2 v_1^2. \quad (3.23)$$

Such a background configuration spontaneously breaks all space-time isometries, if the parameters λ_0 and κ_0 are non-vanishing. The dynamics of fluctuations has interesting features, above all in the tensor sector. Using the same definition for tensor fluctuations as in eq (3.14), we find the following quadratic action for tensor modes

$$S_\gamma^{(2)} = \int dt d^3x a^3 \frac{\mathcal{N}_T}{2} \left[\dot{\gamma}_{ij}^2 - c_T^2 (\partial_k \gamma_{ij})^2 - m_T^2 \gamma_{ij}^2 \right], \quad (3.24)$$

² We also checked that renouncing to this condition one finds a system where ω acquires a healthy dynamics free of Ostrogradsky instabilities (for suitable choices of parameters).

where the parameters entering in the action are

$$\mathcal{N}_T = \frac{M_{Pl}^2 (18H_0^2 + 12v_1^2 + M_{Pl}^2 \lambda_0^2 (q_C - 9\lambda_0^2 q_B))}{18H_0^2 (3 - c_T^2)}, \quad (3.25)$$

$$c_T^2 = \frac{36H_0^2 - 12v_1^2 - M_{Pl}^2 \lambda_0^2 (q_C + 18q_A + 27q_B \lambda_0^2)}{36H_0^2 + 12v_1^2 + M_{Pl}^2 \lambda_0^2 (q_C - 6q_A - 21q_B \lambda_0^2)}, \quad (3.26)$$

$$m_T^2 = \frac{4(3 - c_T^2) M_{Pl}^2 H_0^2 \lambda_0^2 (q_C + 9q_B \lambda_0^2)}{18H_0^2 + 12v_1^2 + M_{Pl}^2 \lambda_0^2 (q_C - 9q_B \lambda_0^2)}. \quad (3.27)$$

We recover the standard result setting $v_1 = \lambda_0 = 0$. The spontaneous breaking of space isometries allows for a mass term for tensor fluctuations. It can be positive or negative, depending on the sign and on the size of the parameters q_C, q_B, v_1^2 . Tensor fluctuations are not adiabatic modes in our scenario, hence they are not necessarily conserved at superhorizon scales: if $m_T^2 > 0$, we find a *blue spectrum* ($n_T > 0$) for primordial gravitational waves. We want to recall that also the original set-up of solid inflation finds a blue spectrum for tensor modes: the spectral tilt in that case is however proportional to slow-roll parameters, hence its size is small. In our scenario, we have more freedom to choose a parametrically larger value for the tensor parameters.

The dynamics of scalar fluctuations is also relevant for our arguments. As usual, we need to satisfy ADM constraints [29], which we discuss in Appendix A. In a convenient unitary gauge for the field ϕ , we find a single propagating scalar mode, the field A in eq (3.10), and the corresponding quadratic action reads

$$S_A^{(2)} = \frac{\mathcal{N}_A}{2} \int d^4x a^3 \left[\dot{A}^2 - c_A^2 (\partial_i A)^2 - m_A^2 A^2 \right]. \quad (3.28)$$

The quantities \mathcal{N}_A, c_A, m_A are constant parameters given by

$$\mathcal{N}_A = 12 \frac{(1 - c_T^2)^2}{(2 - c_T^2)^2} \mathcal{N}_T, \quad (3.29)$$

$$c_A^2 = \frac{2 - c_T^2}{3}, \quad (3.30)$$

$$m_A^2 = m_T^2 \frac{9(2 - c_T^2)^2 q_B \lambda_0^2}{(1 - c_T^2)^2 (2q_C + 27q_B \lambda_0^2)}. \quad (3.31)$$

For make easier comparison, we expressed the results using the tensor quantities \mathcal{N}_T, c_T, m_T defined in equations (3.25), (3.26) and (3.27). As long as \mathcal{N}_T is positive, the overall coefficient \mathcal{N}_A of scalar fluctuations is positive (or at most vanishing when $c_T = 1$): we can have a positive squared mass for the tensor modes in pure de Sitter space, without ghosts in the scalar sector, evading the Higuchi bound. This is a relevant feature of our scenario. We interpret this result as due to non-minimal interactions of scalar fields with gravity, which allow us to find a de Sitter background with non-vanishing background *vevs* for the scalar fields. Those *vevs* spontaneously break all de Sitter symmetries, including the symmetries crucial to prove the existence of the Higuchi ghost [15], as pointed out in [34]. Hence, in our set-up with large couplings between tensor fluctuations and the fields driving accelerated expansion, it is possible to consistently have tensor fluctuations around pure de Sitter with masses in the interval $0 < m_T^2 < 2H_0^2$.

It would also be interesting to consider higher order (e.g. cubic) interactions for scalar modes, to estimate the strong coupling scale in this system, as well as possible interesting features in scalar interactions.

4 Phenomenological consequences

In this section we discuss the phenomenological consequences of our previous findings for what respects tensor modes, both at the level of power spectrum and bispectrum. We only focus on the tensor sector, although a system with broken space reparameterizations can have interesting consequences also for correlation functions involving the scalar sector (see e.g. [13, 25, 35–40] and [41]). We are interested to consider a set-up where the primordial tensor power spectrum increases towards small scales: it is unobservable at CMB scales, but it can be relevant at frequencies probed by interferometers (10^{-4} Hz $\lesssim f \lesssim 10^3$ Hz), where primordial scalar fluctuations are not important. To reduce the number of parameters, we choose $c_T = 1$, $\lambda_0 = 1$, and $q_B = 0$ (while we continue to satisfy the condition (3.21)). This choice “switches off” completely the scalar sector at quadratic level (see eq (3.29)), and we are left with phenomenologically rich set up for tensor fluctuations around de Sitter space. The system still spontaneously breaks time and space reparameterizations: given the conditions we have analysed in the previous Section, and the fact that $\lambda_0 = 1$, we can take as symmetry breaking parameters the quantities κ_0 and m_T , or alternatively the parameters q_A , q_C which appear in the initial action (2.1).

We start discussing the consequences of our findings for the scale dependence of the tensor spectrum that, as we have mentioned above, can have a positive tensor tilt and can be detectable with interferometers as LISA [42] (see also [43] for the first investigations on the possibility of direct detection of primordial gravitational waves). Then we continue discussing how our system, which allows for large tensor non-Gaussianity enhanced in the squeezed limit, can induce a quadrupolar anisotropy in the tensor power spectrum.

4.1 Tensor blue spectrum: inflationary tensor modes at interferometers

When $c_T = 1 = \lambda_0$, and $q_B = 0$, the quadratic action for tensor modes can be expressed as

$$S_\gamma^{(2)} = \frac{\bar{M}_{Pl}^2}{4} \int dt d^3x a^3 \left[\dot{\gamma}_{ij}^2 - (\partial_k \gamma_{ij})^2 - m_T^2 \gamma_{ij}^2 \right]. \quad (4.1)$$

The effective Planck mass is given by

$$\bar{M}_{Pl}^2 = M_{Pl}^2 \left(1 - \frac{q_A M_{Pl}^2}{3H_0^2} \right), \quad (4.2)$$

while the tensor mass squared reads

$$m_T^2 = \frac{4H_0^2 M_{Pl}^2 q_C}{9H_0^2 - 3q_A M_{Pl}^2}. \quad (4.3)$$

These quantities depend on the two parameters q_A and q_C that are associated to the breaking of space reparameterization: when they are set to zero, we recover the standard results for tensor fluctuations around a de Sitter background [30].

We expand tensor fluctuations in Fourier space as

$$\gamma_{ij}(t, \vec{x}) = \int \frac{d^3k}{(2\pi)^3} \tilde{\gamma}_{ij}(t, \vec{k}) e^{i\vec{k}\cdot\vec{x}}. \quad (4.4)$$

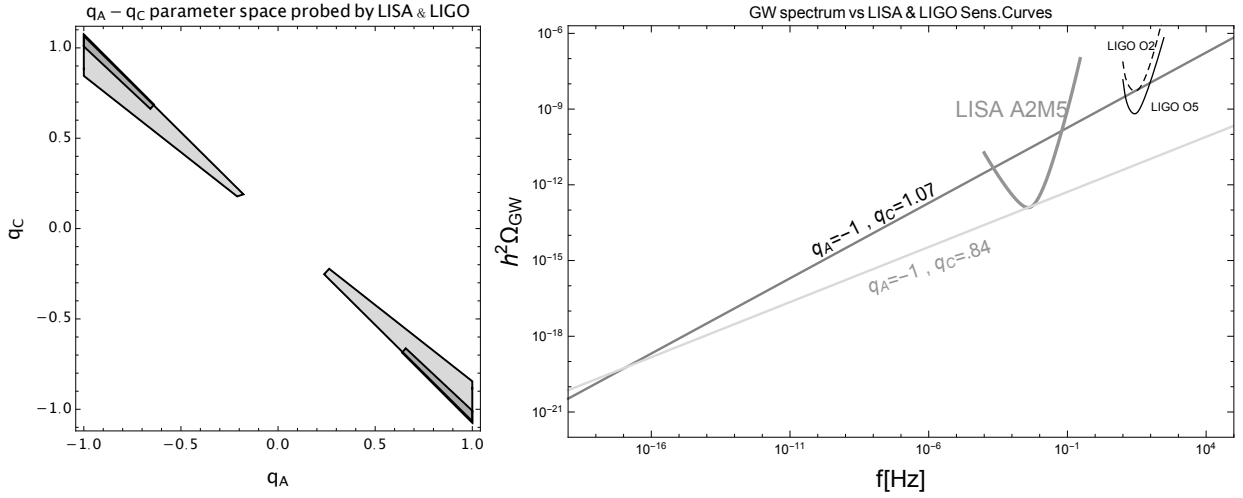


Figure 1. Left: Parameter space probed by LISA and LIGO for q_A - q_C parameters. The lighter gray region is the region probed by LISA in the A2M5 (5 years mission, 2 million armlength). While the darker gray is the region probed by LIGO considering a detection in the O5 run. The plot is obtained for $H = 10^{12}$ GeV. **Right:** Spectrum of GWs energy density $h^2\Omega_{gw}$ for different values of q_A and q_C parameters, compared with the sensitivity of LISA A2M5 (gray curves) and Advanced LIGO (black curves) detectors. We use $k_* = 0.002$ Mpc $^{-1}$ as a pivot scale.

The Fourier mode $\tilde{\gamma}_{ij}$ can be quantized and decomposed in terms of polarization tensors, and creation/annihilation operators

$$\tilde{\gamma}_{ij} = \sum_s \left[\gamma_k \mathbf{e}_{ij}^{(s)}(\vec{k}) a_s(\vec{k}) + \gamma_{-k}^* \mathbf{e}_{ij}^{*(s)}(-\vec{k}) a_s^\dagger(-\vec{k}) \right], \quad (4.5)$$

with $\mathbf{e}_{ij}^{(s)}$ indicating the polarization tensor with helicity $s = \pm 2$, satisfying the transverse-traceless condition $k_i \mathbf{e}_{ij}^{(s)} = \mathbf{e}_{ii}^{(s)} = 0$. We adopt the normalization conditions: $\mathbf{e}_{ij}^{(s)} \mathbf{e}_{ij}^{(s')} = \delta_{ss'}$. We also use the following property $\mathbf{e}_{ij}^{*(s)}(\vec{k}) = \mathbf{e}_{ij}^{(-s)}(\vec{k}) = \mathbf{e}_{ij}^{(s)}(-\vec{k})$. The creation/annihilation operators satisfy the usual commutation relations $[a_s(\vec{k}), a_{s'}^\dagger(\vec{k}')] = (2\pi)^3 \delta_{ss'} \delta^{(3)}(\vec{k} - \vec{k}')$.

Quantization proceeds in a textbook manner [44], and one finds the following expression for the tensor power spectrum $\mathcal{P}_\gamma = (k^3/4\pi^2) \langle \gamma^s \gamma^s \rangle$ (the two-point (2-pt) function has the same amplitude for each of the two polarizations + and \times)

$$\mathcal{P}_\gamma = \frac{H_0^2}{\bar{M}_{Pl}^2} \frac{2^{2\nu-2}}{\pi^2} \left(\frac{k}{k_*} \right)^{3-2\nu}, \quad (4.6)$$

where \bar{M}_{Pl} is the renormalized Planck mass (4.2), the tensor spectral tilt $n_T \equiv \left. \frac{d \ln \mathcal{P}_h}{d \ln k} \right|_{k=k_*} = 3 - 2\nu$ and

$$\nu = \sqrt{\frac{9}{4} - \frac{m_T^2}{H_0^2}}. \quad (4.7)$$

We then find that in our set-up, when $m_T^2 > 0$ and hence $(3-2\nu) > 0$, we can have a power spectrum for tensor modes which increases towards small scales (a blue spectrum), where interferometers like LISA [42] and LIGO-Virgo are sensitive [45]. In Fig. 1 we represent the capability of experiments like LISA and

Advanced LIGO (run O2 and future O5) to probe the parameter space of the model under analysis. In particular, on the left plot, we show how a LISA configuration with 5 years mission and 2 million km arm-length (which is the one closely similar to the ESA approved one), can probe the parameters of our specific inflationary model. We can also appreciate how LISA is sensitive to a larger range of parameters compared to LIGO. In the right plot we have plotted the GW energy density for some representative values of the parameters q_A and q_C versus the LISA and Advanced LIGO sensitivities. The fractional GW energy density is related to the power spectrum (4.6) by the transfer function (see e.g. [1, 46] for more details). Our scenario allows for an increasing GW power on small scales, and its amplitude results well within LISA sensitivity curves.

4.2 Tensor squeezed non-Gaussianity and anisotropic tensor power spectrum

Since tensor modes are non-adiabatic in this system, we expect important consequences for tensor interactions and, in particular, for primordial tensor non-Gaussianity, including a possible violation of Maldacena’s consistency condition [18]. We discuss this subject in this section, analysing implications for the tensor power spectrum.

The action for tensor fluctuations expanded to cubic order is (we choose as above $c_T = 1$, $q_B = 0$)

$$S_\gamma^{(3)} = \frac{\bar{M}_{Pl}^2}{4} \int dt d^3x a^3 \left[\frac{\mathcal{C}_1}{a^2} \gamma_{ij} \gamma_{nm} \left(\partial_j \partial_n \gamma_{im} - \frac{1}{2} \partial_i \partial_j \gamma_{mn} \right) + \mathcal{C}_2 \gamma_{ij} \gamma_{jm} \gamma_{mi} \right], \quad (4.8)$$

where the two coefficients \mathcal{C}_1 and \mathcal{C}_2 are equal to

$$\mathcal{C}_1 = 1 + \frac{M_{Pl}^2}{36 H_0^2} (q_C - 30q_A), \quad (4.9)$$

$$\mathcal{C}_2 = \frac{2 M_{Pl}^2}{27} (4q_C + 9q_A). \quad (4.10)$$

Action (4.8) is weighted by the renormalized Planck mass \bar{M}_{Pl}^2 of eq (4.2). The first part of action (4.8), weighted by the parameter \mathcal{C}_1 , has the very same structure as the third order action of tensor modes in General Relativity (see e.g. [18, 47]), but the overall coefficient is different. In the limit where we restore space reparameterization invariance, setting $q_A = q_C = 0$, we find $\mathcal{C}_1 = 1$, which is the General Relativity result. However in general, given our freedom to choose the parameter q_A , q_C we can have parametrically large deviations from $\mathcal{C}_1 = 1$. The second contribution to action (4.8), weighted by \mathcal{C}_2 , is absent in GR and in any single field inflation model, and is characteristic of theories which break space diffeomorphisms: when $q_A = q_C = 0$, we find $\mathcal{C}_2 = 0$.

A distinctive feature of the cubic operators contained in action (4.8) is that they lead to tensor non-Gaussianity (nG) with shape peaked in the squeezed limit (in contrast with the “equilateral shape” tensor nG characteristic of systems with particle production, see e.g. [5, 49, 50], or models of single field inflation [18, 47, 51]). This subject has been developed in our previous paper [17] to which we refer the reader for more details: here we only present in Fig. 2 a plot of the shape function of the bispectrum (Fourier transform of the 3-pt correlation function) for tensor modes, associated with the operator proportional to \mathcal{C}_1 , whose shape is manifestly peaked in the squeezed limit. We reiterate that its amplitude can be parametrically larger than in GR, by choosing appropriately the parameters q_A , q_C .

Tensor non-Gaussianity might appear as a futuristic observable well beyond the sensitivity of planned experiments. However a large non-Gaussian amplitude peaked in the squeezed limit can induce a large

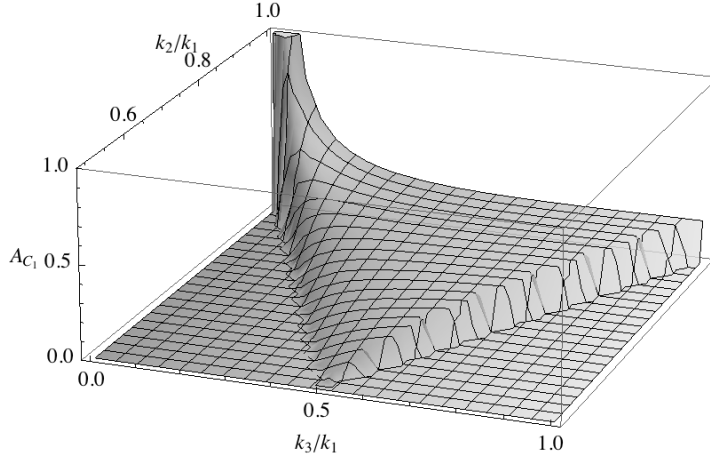


Figure 2. Plot of the shape function of the tensor bispectrum for the term proportional to \mathcal{C}_1 : $\mathcal{A}_{\mathcal{C}_1}^{+++}(1, k_2/k_1, k_3/k_1)(k_2/k_1)^2(k_3/k_1)^2$ as a function of k_2/k_1 and k_3/k_1 . The plot is normalized to unity for equilateral configurations $k_2/k_1 = k_3/k_1 = 1$.

quadrupolar anisotropy in the tensor power spectrum, leading to a possible estimator for tensor non-Gaussianity. Indeed, we can write the following general expression for the squeezed limit of the tensor 3-pt function

$$\lim_{\bar{q} \rightarrow 0} \langle \gamma_{\bar{q}}^{s_1} \gamma_{\vec{k}}^{s_2} \gamma_{-\vec{k}}^{s_3} \rangle' = \delta^{s_2 s_3} \mathcal{P}_\gamma(q) \mathcal{P}_\gamma(k) \left(\frac{3}{2} + f_{\text{NL}}^T \right) \mathbf{e}_{ij}^{(s_1)}(\bar{q}) \frac{k^i k^j}{k^2}. \quad (4.11)$$

where q and k represent the momenta of the *long* and *short* tensor mode, respectively. The non-linear parameter f_{NL}^T characterises how much we are departing from the standard consistency relation, due to non-adiabaticity of tensor modes. For example in our case, setting $\mathcal{C}_2 = 0$, f_{NL}^T is proportional to $(\mathcal{C}_1 - 1)$, which can be parametrically larger than unity. In the presence of large squeezed tensor non-Gaussian signal, a single long wavelength tensor mode – which we denote with a bar as $\bar{\gamma}_{\bar{q}}^s$ – modulates the tensor two-point function as follows [34, 48]

$$\langle \gamma_{\vec{k}}^{s_1} \gamma_{-\vec{k}}^{s_2} \rangle'_{\bar{\gamma}} = \langle \gamma_{\vec{k}}^{s_1} \gamma_{-\vec{k}}^{s_2} \rangle'_0 + \bar{\gamma}_{\bar{q}}^{s_3} \frac{\langle \bar{\gamma}_{\bar{q}}^{s_3} \gamma_{\vec{k}}^{s_1} \gamma_{-\vec{k}}^{s_2} \rangle'}{\mathcal{P}_\gamma(q)}, \quad \text{for } q \ll k. \quad (4.12)$$

We denote with $\langle \dots \rangle'_{\bar{\gamma}}$ the n-pt function modulated by the long tensor mode, while with $\langle \dots \rangle'_0$ the unmodulated quantity (the prime means that we do not include the momentum conserving δ -function in these expressions).

Physically, we should consider the cumulative effect of *all* soft graviton modes whose momenta are smaller than a representative momentum q_L , which is proportional to the inverse of the size of the instrument we use to detect tensor modes; in the extreme case, the size of the apparatus can be the entire observable universe, of order H^{-1} . At a given position \vec{x} , we can write (see e.g. [53])

$$\langle \gamma_{\vec{k}_1}^{s_1} \gamma_{\vec{k}_2}^{s_2} \rangle'_{\bar{\gamma}}(\vec{x}) = \langle \gamma_{\vec{k}_1}^{s_1} \gamma_{\vec{k}_2}^{s_2} \rangle'_0 + \frac{1}{V_L} \int_{|\bar{q}| < q_L} d^3 q e^{i\bar{q} \cdot \vec{x}} \left(\sum_{s_3 = +, \times} \bar{\gamma}_{\bar{q}}^{s_3} \frac{\langle \bar{\gamma}_{\bar{q}}^{s_3} \gamma_{\vec{k}_1}^{s_1} \gamma_{\vec{k}_2}^{s_2} \rangle'}{\mathcal{P}_\gamma(q)} \right), \quad (4.13)$$

with V_L the volume (in Fourier space) of the space of 3-momenta over which we are integrating. We can substitute above the expression for the squeezed limit of the 3-pt function, eq (4.11), and we get

$$\langle \gamma_{\vec{k}}^{s_1} \gamma_{-\vec{k}}^{s_2} \rangle'_{\bar{\gamma}}(\vec{x}) = \langle \gamma_{\vec{k}}^{s_1} \gamma_{-\vec{k}}^{s_2} \rangle'_0 \left(1 + f_{NL}^T \frac{k^i k^j}{k^2} \frac{1}{V_L} \int_{|\vec{q}| < q_L} d^3 q e^{i\vec{q} \cdot \vec{x}} \sum_{s_3} \mathbf{e}_{ij}^{(s_3)}(\vec{q}) \bar{\gamma}_q^{(s_3)} \right), \quad (4.14)$$

$$= \langle \gamma_{\vec{k}}^{s_1} \gamma_{-\vec{k}}^{s_2} \rangle'_0 \cdot \left(1 + \frac{k^i k^j}{k^2} \mathcal{Q}_{ij}(\vec{x}) \right), \quad (4.15)$$

where we have introduced the quantity

$$\mathcal{Q}_{ij}(\vec{x}) = \frac{f_{NL}^T}{V_L} \int_{|\vec{q}| < q_L} d^3 q e^{i\vec{q} \cdot \vec{x}} \sum_s \mathbf{e}_{ij}^{(s)}(\vec{q}) \bar{\gamma}_q^{(s)}. \quad (4.16)$$

Hence eq (4.15) implies that the tensor power spectrum can acquire a position-dependent quadrupolar asymmetry, due the coupling between long and short wavelength tensor fluctuations in the primordial universe. The quantity \mathcal{Q}_{ij} acquires stochastic random values over a Gaussian distribution, with variance that depends on the nG parameter appearing in eq (4.11) (see e.g. [34]):

$$\langle \mathcal{Q}_{ij} \mathcal{Q}_{ij} \rangle = \frac{4\pi}{V_L^2} (f_{NL}^T)^2 \sum_s \int_{q < q_L} dq q^2 \langle \bar{\gamma}_{\vec{q}}^{(s)} \bar{\gamma}_{-\vec{q}}^{(s)} \rangle'. \quad (4.17)$$

As discussed in the previous subsection, we are interested in a situation where the tensor tilt n_T is positive, implying that the integral in eq (4.17) converges in the infrared domain. Notice that although the tensor 2pt function acquires a quadrupolar anisotropy, still this effect is the same for both polarizations $+$ and \times , and we do not have any cross correlation among polarizations: this is due to the fact that the background is still isotropic (being de Sitter space), and the effect described above is only due to the coupling between long and short modes, which is induced by non-Gaussianity. As a consequence, the tensor power spectrum can be parameterized as

$$\mathcal{P}_{\bar{\gamma}}(k) = \mathcal{P}_0(k) \left(1 + \mathcal{Q}_{ij} \frac{k^i k^j}{k^2} \right). \quad (4.18)$$

where $\mathcal{P}_0(k)$ represents the standard isotropic contribution to the tensor power spectrum. In order to characterize the SGWB, since GWs have two polarizations, is common to expand them in terms of Stokes parameters, by analogy with electromagnetic cases; these make more clear the properties and symmetries of GW polarizations. In particular, in our specific case, when the tensor two point function is decomposed in terms of Stokes parameters the only non-vanishing parameter appears to be the intensity I of GWs, characterised by a quadrupolar anisotropy controlled by the quantity \mathcal{Q}_{ij} . The other Stokes parameters V, U and Q are zero: the first because in this case we do not have any asymmetry in the two polarization amplitudes of the GWs, typical of models that violate parity symmetry [52]; Q and U because they carry additional information about linear polarizations, in particular about cross correlations among polarizations which are absent in our specific case.

4.3 Interferometer response to an anisotropic tensor power spectrum

For the rest of this section, we briefly start to explore consequences of the results found so far, for what respect the power spectrum of primordial tensor modes detectable with gravitational wave interferometers. We use the methods first discussed in [54], and developed in various works as [55, 57, 58]. We follow

closely [57], extending their results to describe our set-up, which includes an anisotropic tensor power spectrum.

We focus our attention only on the consequences of tensor anisotropies of the form of eq (4.18) for the relative phase shift of light which travels between test masses located at the extremes of the arms of an interferometer. We postpone a more detailed analysis on the physical implications and characterisation of the GW signal to future publications.

It is convenient to expand gravitational wave modes in plane waves, implementing an interferometer notation (see e.g. [59])

$$\gamma_{ij}(t, \vec{x}) = \int_{-\infty}^{+\infty} df \int d^2\vec{n} \sum_s \gamma^{(s)}(f, \vec{n}) \mathbf{e}_{ij}^{(s)} e^{i2\pi f(t - \vec{n} \cdot \vec{x})}, \quad (4.19)$$

with f the frequency, and \vec{n} the versor in the direction of 3-momentum of the propagating wave. In our specific set-up, the 2-pt function for the mode function appearing the previous expansion reads

$$\langle \gamma^{(s)}(f, \vec{n}), \gamma^{(s')}(f', \vec{n}') \rangle = \frac{\delta(f - f')}{2} \frac{\delta^{(2)}(\vec{n} + \vec{n}')}{4\pi} \delta^{ss'} S_\gamma(f) (1 + \mathcal{Q}_{mn} n^m n^n), \quad (4.20)$$

where $S_\gamma(f)$ is the amplitude of the intensity signal, which depends on the amplitude of the primordial tensor spectrum

$$S_\gamma(f) = \frac{H_0^2}{\bar{M}_{Pl}^2 f^3} \frac{2^{2\nu-2}}{\pi^2} \left(\frac{f}{f_*} \right)^{3-2\nu}, \quad (4.21)$$

with ν defined in eq (4.7), while \mathcal{Q}_{mn} is the anisotropic contribution to the tensor power spectrum defined in eq (4.16). For simplicity, in this work we make the hypothesis that the quantity \mathcal{Q}_{mn} is constant, and independent from the position of the interferometer. This situation occurs for example if the spatial dependence of the long wavelength tensor mode controlling \mathcal{Q}_{mn} is weak within the horizon corresponding to region of space containing the instrument (for example the solar system in the case of LISA).

We model an interferometer as made of n arms, with test masses M_i at their extremes ($i = 1, \dots, 2n$), located at position \vec{x}_i . The basic quantity which controls how the interferometer responds to a gravitational wave is the electromagnetic phase shift accumulated by light during its travelling along an arm of the instrument:

$$\phi_{12}(t) = \phi_0 \left[1 + \int_{-\infty}^{+\infty} df \int d^2\vec{n} \sum_s \gamma^{(s)} \mathbf{e}_{ab}^{(s)} e^{i2\pi f(t - \vec{n} \cdot \vec{x}_1)} \mathcal{D}_{ab}(f, \vec{\ell}_{12} \cdot \vec{n}) \right], \quad (4.22)$$

with \vec{x}_1 the location of mass M_1 , and $\vec{x}_2 = \vec{x}_1 + L \vec{\ell}_{12}$ the location of mass M_2 ($\vec{\ell}_{12}$ being the unit vector in the direction of the interferometer arm). ϕ_0 is the phase measured in absence of a gravitational wave passing through the arms of the interferometer. The quantity $\mathcal{D}_{ab}(f, \vec{\ell}_{12} \cdot \vec{n})$ is the arm transfer function

$$\mathcal{D}_{ab}(f, \vec{\ell} \cdot \vec{n}) = \frac{1}{2} \ell_a \ell_b \mathcal{M}(f, \vec{\ell} \cdot \vec{n}), \quad (4.23)$$

with \mathcal{M} given by

$$\mathcal{M}(\vec{\ell} \cdot \vec{n}, f) \equiv \frac{i}{2\pi L_D f} \frac{\exp\left[2\pi i L_D f (1 - \vec{\ell} \cdot \vec{n})\right] - 1}{1 - \vec{\ell} \cdot \vec{n}},$$

and $1/(2\pi L_D)$ is the characteristic frequency scale of the detector. The signal $s_1(t)$, associated with the interferometer arm, is defined in terms of the phase shift of the electromagnetic wave as it travels from one end of the arm to the other, and back [58]

$$s_1(t) = \phi_{12}(t - 2L) + \phi_{21}(t - L) + n_1(t), \quad (4.24)$$

where with ϕ_{12} and ϕ_{21} we indicate the shifts and with $n_1(t)$ a noise term. Hence we learn that the signal is built in terms of a linear combination of phase shifts: it is essential to specify the properties of the latter, in order to deduce implications for the former.

It is convenient to work with the Fourier transform of the phase shift accumulated along any of the interferometer arms:

$$\Delta\tilde{\phi}_{ij}(f) = \int d^2\vec{n} \sum_s \gamma^{(s)} \mathbf{e}_{ab}^{(s)} e^{-i2\pi f\vec{n}\cdot\vec{x}_1} \mathcal{D}_{ab}(f, \vec{\ell}_{ij} \cdot \vec{n}). \quad (4.25)$$

To extract information about the stochastic GW background we need to correlate two phase shifts, so, using eq (4.20), we find that the 2-pt function of the phase shift reads as

$$\langle \Delta\tilde{\phi}_{ij}(f) \Delta\tilde{\phi}_{kl}^*(f') \rangle = \frac{1}{2} \delta(f - f') \delta^{ss'} S_h(f) \mathcal{R}_{ss'}^{ij,kl}(f), \quad (4.26)$$

where the quantity $\mathcal{R}_{ss'}^{ij,kl}(f)$ is the response function of the interferometer to a gravitational wave passing through its arms. In our specific case it acquires a new contribution with respect to the standard case where just an isotropic stochastic signal is present [56, 57], which we collect in the second line of the following expression

$$\begin{aligned} \mathcal{R}_{ss'}^{ij,kl}(f) &\equiv \int \frac{d^2\vec{n}}{4\pi} e^{i2\pi f\vec{n}(\vec{x}_i - \vec{x}_k)} \mathcal{D}_{ab}(\vec{\ell}_{ij} \cdot \vec{n}, f) \mathbf{e}_{ab}^{(p)}(\vec{n}) \mathcal{D}_{cd}^*(\vec{\ell}_{kl} \cdot \vec{n}, f) \mathbf{e}_{cd}^{(p')}(\vec{n}') \\ &+ \mathcal{Q}_{mn} \int \frac{d^2\vec{n}}{4\pi} n_m n_n e^{i2\pi f\vec{n}(\vec{x}_i - \vec{x}_k)} \mathcal{D}_{ab}(\vec{\ell}_{ij} \cdot \vec{n}, f) \mathbf{e}_{ab}^{(p)}(\vec{n}) \mathcal{D}_{cd}^*(\vec{\ell}_{kl} \cdot \vec{n}, f) \mathbf{e}_{cd}^{(p')}(\vec{n}). \end{aligned} \quad (4.27)$$

The contribution proportional to the tensor \mathcal{Q}_{mn} , in the second line of the previous formula, quantifies how the quadrupolar anisotropy affects the interferometer response. In this way the response function is given by the sum of two contributions

$$\mathcal{R}_{ss'}^{ij,kl}(f) \equiv {}^{(0)}\mathcal{R}_{ss'}^{ij,kl}(f) + {}^{(1)}\mathcal{R}_{ss'}^{ij,kl,mn}(f) \mathcal{Q}_{mn}. \quad (4.28)$$

The first part, ${}^{(0)}\mathcal{R}$, is the standard contribution discussed in [57]. The second part, proportional ${}^{(1)}\mathcal{R}$, characterises a new contribution modulated by the squeezed non-Gaussianity. The integrals in eq (4.27) depend on the positions \vec{x}_i and \vec{x}_k of the masses M_i and M_k of the interferometer, as well as on the orientation of the interferometer with respect to the ‘‘preferred directions’’ controlled by the tensorial quantity \mathcal{Q}_{mn} . This latter quantity depends on the amplitude of long-wavelength graviton modes whose wavelength is larger than the size of the instrument used to make the measurement. For the case of LISA interferometer configuration, for example, such size is the solar system.

Collecting these results, we find that the two-point function among the phase shifts reads

$$\langle \Delta\tilde{\phi}_{ij}(f) \Delta\tilde{\phi}_{kl}^*(f) \rangle = \frac{\delta^{ss'} S_h(f)}{2} {}^{(0)}\mathcal{R}_{ss'}^{ij,kl}(f) + \frac{\delta^{ss'} S_h(f)}{2} \mathcal{Q}_{mn} {}^{(1)}\mathcal{R}_{ss'}^{ij,kl,mn}(f). \quad (4.29)$$

The second term contains the anisotropic contribution associated with tensor nG , and it is a distinctive feature of our system. The value of this contribution depends on how the interferometer arm vectors $\vec{\ell}_{ij}$ are oriented with respect to the long wavelength tensor mode, through the quantity \mathcal{Q}_{mn} . Interestingly, while the first term in (4.29) is constant in time (as long as the relative orientation of the interferometer arms do not change) the value of the second contribution in (4.29) can depend on time, since the orientation of the interferometer arms changes with respect to \mathcal{Q}_{mn} as time passes: few hours for earth-based interferometers (e.g. LIGO-Virgo), or few months for space interferometers, like LISA.

This fact can lead to distinctive observational consequences. The two-point phase shift correlation is the basic ingredient for building signal estimators for gravitational wave detection at interferometers [54, 55, 57, 58], in terms of correlation functions of the signal. A measurement of a time-dependent modulation for a stochastic primordial tensor spectrum, whose amplitude changes with time (within months for an interferometer like LISA), can be a smoking gun for large non-Gaussianity in the tensor sector. On the contrary, bounds on time variations of the amplitude of the stochastic signal can be used to impose bounds on the size of non-Gaussianity parameters, like f_{NL}^T . We plan to return to discuss in detail phenomenological consequences of these results in a separate publication.

5 Discussion

In this paper we have developed a system of supersolid inflation, where time and space reparameterizations are spontaneously broken by the background $vevs$ of a set of scalar fields coupled to gravity. We shown that this scenario has distinctive features for the properties of primordial tensor modes. The primordial tensor spectrum can have a blue tilt with parametrically large value of the tensor tilt n_T . The Higuchi bound can be avoided thanks to interactions between the tensor perturbations and the fields driving inflation. Tensor modes are not adiabatic in this set-up. This system can have large tensor non-Gaussianities enhanced in the squeezed limit, which couple long and short tensor fluctuations, leading to a quadrupolar anisotropy in the tensor power spectrum. We have discussed phenomenological consequences of our findings, in particular their implications for interferometer searches of a primordial stochastic gravitational wave background. We shown that a future space-based interferometer mission like LISA can probe (and constrain) parameters of our model. We have briefly discussed how a quadrupolar anisotropy in the tensor power spectrum can lead to a time dependent modulation of the amplitude of a SGWB. This fact can in principle allow one to build a specific estimator for testing squeezed tensor non-Gaussianities, to be used with future interferometers.

Acknowledgments

It is a pleasure to thank Marco Peloso for useful discussions. We also would like to acknowledge the LISA Cosmology working group for discussions, and for feedback on a presentation of these results during the IV LISA workshop in Mainz. The work of GT is partially supported by the STFC grant ST/P00055X/1.

A ADM constraints for scalar perturbations

In this Appendix we discuss the constraint conditions for the scalar sector of the supersolid inflation system described in Section 3.2. The background metric and scalar fields are

$$ds^2 = -dt^2 + e^{2H_0 t} d\vec{x}^2, \quad (\text{A.1})$$

$$\phi = \kappa_0^2 t, \quad (\text{A.2})$$

$$\sigma^I = \lambda_0 x^I. \quad (\text{A.3})$$

We choose the parameter q_ϕ as

$$q_\phi = \frac{(q_A + 2q_B \lambda_0^2)}{q_\sigma}. \quad (\text{A.4})$$

The branch of background solutions we are interested in determines the following choice for the available parameters

$$H_0^2 = \frac{M_{Pl}^2}{6 q_\sigma} (q_A + 2q_B \lambda_0^2), \quad (\text{A.5})$$

$$\kappa_0^2 = \frac{M_{Pl}^4}{6} (q_C - 9q_B \lambda_0^4) + 2M_{Pl}^2 v_1^2, \quad (\text{A.6})$$

In order to study scalar fluctuations, we implement a partial unitary gauge, the same as in our work [13]. We leave the scalar ϕ unperturbed, while we perturb metric and scalars σ^I as

$$ds^2 = -(1 + 2N) dt^2 + 2 e^{2H_0 t} \partial_i B dx^i dt + e^{2H_0 t} (1 + 2A) \delta_{ij} dx^i dx^j, \quad (\text{A.7})$$

$$\sigma^I = \lambda_0 x^I + \frac{\lambda_0}{\sqrt{-\nabla^2}} \partial^I \omega. \quad (\text{A.8})$$

The equations of motion for N , B , ω correspond to constraint equations, which lead to the following solutions in momentum space

$$N = \frac{\dot{A}}{H_0 (2 - c_T^2)}, \quad (\text{A.9})$$

$$B = - \frac{\left[3 (1 - c_T^2)^2 a^2 H_0 \dot{A} + (2 - c_T^2) k^2 A \right]}{(2 - c_T^2)^2 H_0 a^2 k^2}, \quad (\text{A.10})$$

$$\omega = - \left(\frac{27 q_B \lambda_0^4}{k (2q_C + 27q_B \lambda_0^4)} \right) A, \quad (\text{A.11})$$

with c_T given in eq (3.26). Substituting these expressions in the action, we find that the scalar dynamics corresponds to a single field scenario, controlled by the quadratic action (3.28).

References

- [1] M. Maggiore, Phys. Rept. **331** (2000) 283 [gr-qc/9909001].
- [2] M. Guzzetti, C., N. Bartolo, Liguori, M. and S. Matarrese, Riv. Nuovo Cim. **39** (2016) no.9, 399 [arXiv:1605.01615 [astro-ph.CO]].
- [3] M. Kamionkowski and E. D. Kovetz, Ann. Rev. Astron. Astrophys. **54** (2016) 227 [arXiv:1510.06042 [astro-ph.CO]].
- [4] J. L. Cook and L. Sorbo, Phys. Rev. D **85** (2012) 023534 [arXiv:1109.0022 [astro-ph.CO]].
- [5] J. L. Cook and L. Sorbo, JCAP **1311** (2013) 047 [arXiv:1307.7077 [astro-ph.CO]].
- [6] M. Biagetti, E. Dimastrogiovanni, M. Fasiello and M. Peloso, JCAP **1504** (2015) 011 [arXiv:1411.3029 [astro-ph.CO]].
- [7] N. Barnaby, E. Pajer and M. Peloso, Phys. Rev. D **85** (2012) 023525 [arXiv:1110.3327 [astro-ph.CO]].
- [8] V. Domcke, M. Pieroni and P. Bintruy, JCAP **1606** (2016) 031 [arXiv:1603.01287 [astro-ph.CO]].
- [9] N. Bartolo *et al.*, JCAP **1612** (2016) no.12, 026 [arXiv:1610.06481 [astro-ph.CO]].
- [10] S. Endlich, A. Nicolis and J. Wang, JCAP **1310** (2013) 011 [arXiv:1210.0569 [hep-th]].
- [11] A. Gruzinov, Phys. Rev. D **70** (2004) 063518 [astro-ph/0404548].
- [12] A. Nicolis, R. Penco and R. A. Rosen, Phys. Rev. D **89** (2014) no.4, 045002 [arXiv:1307.0517 [hep-th]].
- [13] N. Bartolo, D. Cannone, A. Ricciardone and G. Tasinato, JCAP **1603** (2016) no.03, 044 [arXiv:1511.07414 [astro-ph.CO]].
- [14] D. Cannone, G. Tasinato and D. Wands, JCAP **1501** (2015) no.01, 029 [arXiv:1409.6568 [astro-ph.CO]].
- [15] A. Higuchi, Nucl. Phys. B **282** (1987) 397.
- [16] M. Fasiello and A. J. Tolley, JCAP **1312**, 002 (2013) [arXiv:1308.1647 [hep-th]].
- [17] A. Ricciardone and G. Tasinato, Phys. Rev. D **96** (2017) no.2, 023508 [arXiv:1611.04516 [astro-ph.CO]].
- [18] J. M. Maldacena and G. L. Pimentel, JHEP **1109** (2011) 045 [arXiv:1104.2846 [hep-th]].
- [19] R. L. Arnowitt, S. Deser and C. W. Misner, Gen. Rel. Grav. **40** (2008) 1997 [gr-qc/0405109].
- [20] C. Cheung, P. Creminelli, A. L. Fitzpatrick, J. Kaplan and L. Senatore, JHEP **0803** (2008) 014 [arXiv:0709.0293 [hep-th]].
- [21] G. W. Horndeski, Int. J. Theor. Phys. **10** (1974) 363.
- [22] T. Kobayashi, M. Yamaguchi and J. Yokoyama, Phys. Rev. Lett. **105** (2010) 231302 [arXiv:1008.0603 [hep-th]];
T. Kobayashi, M. Yamaguchi and J. Yokoyama, Prog. Theor. Phys. **126** (2011) 511 [arXiv:1105.5723 [hep-th]].
- [23] C. Germani and A. Kehagias, Phys. Rev. Lett. **105** (2010) 011302 [arXiv:1003.2635 [hep-ph]];
C. Germani and A. Kehagias, JCAP **1005** (2010) 019 Erratum: [JCAP **1006** (2010) E01] [arXiv:1003.4285 [astro-ph.CO]].
- [24] P. A. R. Ade *et al.* [Planck Collaboration], Astron. Astrophys. **594** (2016) A16 [arXiv:1506.07135 [astro-ph.CO]].
- [25] G. Domenech, T. Hiramatsu, C. Lin, M. Sasaki, M. Shiraishi and Y. Wang, JCAP **1705** (2017) no.05, 034 [arXiv:1701.05554 [astro-ph.CO]].

- [26] C. Burrage, C. de Rham, D. Seery and A. J. Tolley, *JCAP* **1101** (2011) 014 [arXiv:1009.2497 [hep-th]].
- [27] E. J. Copeland, A. Padilla and P. M. Saffin, *JCAP* **1212** (2012) 026 [arXiv:1208.3373 [hep-th]].
- [28] V. F. Mukhanov, H. A. Feldman and R. H. Brandenberger, *Phys. Rept.* **215** (1992) 203.
- [29] J. M. Maldacena, *JHEP* **0305** (2003) 013 [astro-ph/0210603].
- [30] A. Riotto, *ICTP Lect. Notes Ser.* **14** (2003) 317 [hep-ph/0210162].
- [31] P. Creminelli, J. Gleyzes, J. Norea and F. Vernizzi, *Phys. Rev. Lett.* **113** (2014) no.23, 231301 [arXiv:1407.8439 [astro-ph.CO]].
- [32] D. Baumann, H. Lee and G. L. Pimentel, *JHEP* **1601** (2016) 101 [arXiv:1507.07250 [hep-th]].
- [33] J. Fumagalli, S. Mooij and M. Postma, arXiv:1610.08460 [gr-qc].
- [34] L. Bordin, P. Creminelli, M. Mirbabayi and J. Norea, *JCAP* **1609** (2016) no.09, 041 [arXiv:1605.08424 [astro-ph.CO]].
- [35] E. Dimastrogiovanni, M. Fasiello, D. Jeong and M. Kamionkowski, *JCAP* **1412** (2014) 050 [arXiv:1407.8204 [astro-ph.CO]].
- [36] P. D. Meerburg, J. Meyers, A. van Engelen and Y. Ali-Hamoud, *Phys. Rev. D* **93** (2016) 123511 [arXiv:1603.02243 [astro-ph.CO]].
- [37] S. Endlich, B. Horn, A. Nicolis and J. Wang, *Phys. Rev. D* **90** (2014) no.6, 063506 [arXiv:1307.8114 [hep-th]].
- [38] M. Akhshik, *JCAP* **1505** (2015) no.05, 043 [arXiv:1409.3004 [astro-ph.CO]].
- [39] M. Biagetti, M. Fasiello and A. Riotto, *Phys. Rev. D* **88** (2013) 103518 [arXiv:1305.7241 [astro-ph.CO]].
- [40] M. Biagetti, E. Dimastrogiovanni and M. Fasiello, arXiv:1708.01587 [astro-ph.CO].
- [41] N. Bartolo, S. Matarrese, M. Peloso and A. Ricciardone, *JCAP* **1308** (2013) 022 [arXiv:1306.4160 [astro-ph.CO]];
N. Bartolo, M. Peloso, A. Ricciardone and C. Unal, *JCAP* **1411** (2014) no.11, 009 [arXiv:1407.8053 [astro-ph.CO]]; M. Akhshik, R. Emami, H. Firouzjahi and Y. Wang, *JCAP* **1409** (2014) 012 [arXiv:1405.4179 [astro-ph.CO]]; C. Lin and L. Z. Labun, *JHEP* **1603** (2016) 128 [arXiv:1501.07160 [hep-th]]; D. Cannone, J. O. Gong and G. Tasinato, *JCAP* **1508** (2015) no.08, 003 [arXiv:1505.05773 [hep-th]]; A. A. Abolhasani, M. Akhshik, R. Emami and H. Firouzjahi, *JCAP* **1603** (2016) 020 [arXiv:1511.03218 [astro-ph.CO]]; T. Rostami, A. Karami and H. Firouzjahi, *JCAP* **1706** (2017) no.06, 039 [arXiv:1702.03744 [astro-ph.CO]].
- [42] P. Amaro-Seoane *et al.*, *GW Notes* **6** (2013) 4 [arXiv:1201.3621 [astro-ph.CO]];
- [43] A. R. Liddle, *Phys. Rev. D* **49** (1994) 3805 Erratum: [*Phys. Rev. D* **51** (1995) 4603] [gr-qc/9307036];
R. Bar-Kana, *Phys. Rev. D* **50** (1994) 1157 [astro-ph/9401050];
Phys. Rev. D **55** (1997) R435 [astro-ph/9607066]; T. L. Smith, M. Kamionkowski and A. Cooray, *Phys. Rev. D* **73** (2006) 023504 [astro-ph/0506422].
- [44] D. H. Lyth and A. R. Liddle, Cambridge, UK: Cambridge Univ. Pr. (2009) 497 p
- [45] G. M. Harry [LIGO Scientific Collaboration], *Class. Quant. Grav.* **27** (2010) 084006.
- [46] S. Kuroyanagi, T. Takahashi and S. Yokoyama, *JCAP* **1502** (2015) 003 [arXiv:1407.4785 [astro-ph.CO]].
- [47] X. Gao, T. Kobayashi, M. Yamaguchi and J. Yokoyama, *Phys. Rev. Lett.* **107** (2011) 211301 [arXiv:1108.3513 [astro-ph.CO]].
- [48] K. W. Masui and U. L. Pen, *Phys. Rev. Lett.* **105** (2010) 161302 [arXiv:1006.4181 [astro-ph.CO]]; D. Jeong and M. Kamionkowski, *Phys. Rev. Lett.* **108** (2012) 251301 [arXiv:1203.0302 [astro-ph.CO]]; L. Dai, D. Jeong and M. Kamionkowski, *Phys. Rev. D* **88** (2013) no.4, 043507 [arXiv:1306.3985 [astro-ph.CO]].

- L. Dai, D. Jeong and M. Kamionkowski, Phys. Rev. D **87** (2013) no.10, 103006 [arXiv:1302.1868 [astro-ph.CO]]; S. Brahma, E. Nelson and S. Shandera, Phys. Rev. D **89** (2014) no.2, 023507 [arXiv:1310.0471 [astro-ph.CO]].
- [49] N. Barnaby and M. Peloso, Phys. Rev. Lett. **106** (2011) 181301 [arXiv:1011.1500 [hep-ph]].
- [50] N. Barnaby, R. Namba and M. Peloso, JCAP **1104** (2011) 009 [arXiv:1102.4333 [astro-ph.CO]].
- [51] J. Soda, H. Kodama and M. Nozawa, JHEP **1108** (2011) 067 [arXiv:1106.3228 [hep-th]]; M. Shiraishi, D. Nitta and S. Yokoyama, Prog. Theor. Phys. **126** (2011) 937 [arXiv:1108.0175 [astro-ph.CO]].
- [52] M. Shiraishi, A. Ricciardone and S. Saga, JCAP **1311** (2013) 051 [arXiv:1308.6769 [astro-ph.CO]].
- [53] D. Hanson and A. Lewis, Phys. Rev. D **80** (2009) 063004 [arXiv:0908.0963 [astro-ph.CO]]; S. B. Giddings and M. S. Sloth, JCAP **1101** (2011) 023 [arXiv:1005.1056 [hep-th]]; S. B. Giddings and M. S. Sloth, Phys. Rev. D **84** (2011) 063528 [arXiv:1104.0002 [hep-th]]; S. Nurmi, C. T. Byrnes and G. Tasinato, JCAP **1306** (2013) 004 [arXiv:1301.3128 [astro-ph.CO]]; C. T. Byrnes, S. Nurmi, G. Tasinato and D. Wands, JCAP **1203** (2012) 012 [arXiv:1111.2721 [astro-ph.CO]]; M. Gerstenlauer, A. Hebecker and G. Tasinato, JCAP **1106** (2011) 021 [arXiv:1102.0560 [astro-ph.CO]]; C. T. Byrnes, M. Gerstenlauer, S. Nurmi, G. Tasinato and D. Wands, JCAP **1010** (2010) 004 [arXiv:1007.4277 [astro-ph.CO]]; C. T. Byrnes, M. Gerstenlauer, A. Hebecker, S. Nurmi and G. Tasinato, JCAP **1008** (2010) 006 [arXiv:1005.3307 [hep-th]]; E. Nelson and S. Shandera, Phys. Rev. Lett. **110** (2013) no.13, 131301 [arXiv:1212.4550 [astro-ph.CO]]; M. LoVerde, E. Nelson and S. Shandera, JCAP **1306** (2013) 024 [arXiv:1303.3549 [astro-ph.CO]]. S. Adhikari, S. Shandera and A. L. Erickcek, Phys. Rev. D **93** (2016) no.2, 023524 [arXiv:1508.06489 [astro-ph.CO]].
- [54] N. J. Cornish, Phys. Rev. D **65** (2002) 022004 [gr-qc/0106058].
- [55] R. Kato and J. Soda, Phys. Rev. D **93** (2016) no.6, 062003 [arXiv:1512.09139 [gr-qc]].
- [56] J. D. Romano and N. J. Cornish, Living Rev. Rel. **20** (2017) 2 [arXiv:1608.06889 [gr-qc]].
- [57] T. L. Smith and R. Caldwell, Phys. Rev. D **95** (2017) no.4, 044036 [arXiv:1609.05901 [gr-qc]].
- [58] B. Thorne, T. Fujita, M. Hazumi, N. Katayama, E. Komatsu and M. Shiraishi, arXiv:1707.03240 [astro-ph.CO].
- [59] B. Allen, In *Les Houches 1995, Relativistic gravitation and gravitational radiation* 373-417 [gr-qc/9604033].